UPPSALA
UNIVERSITET

A discontinuous Galerkin local orthogonal decomposition (LOD) method for elliptic multiscale problems

Daniel Elfverson
daniel.elfverson@it.uu.se

Division of Scientific Computing
Uppsala University
Sweden

Outline

Applications of multiscale methods

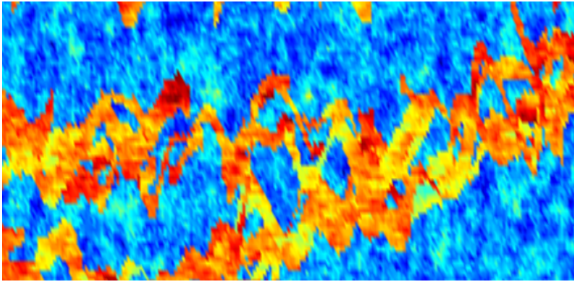

- Subsurface flow
- Composite materials
- ...

Need numerical solution of partial differential equations with rough data (module of elasticity, conductivity, permeability, etc)

Major challenge

Solution has features on a several non-seperal scales

Model problem

Consider the elliptic model problem

$$\begin{aligned} -\nabla \cdot A\nabla u + (\mathbf{b} \cdot \nabla u) &= f \text{ in } \Omega, \\ u &= 0 \text{ on } \partial\Omega, \end{aligned}$$

where we assume:

- $0 < A_{min} \in \mathbb{R} \leq A(x) \in L^\infty(\Omega, \mathbb{R}^{d\times d}_{sym})$
- $f \in L^2(\Omega)$
- $\mathbf{b} \in [W^1_\infty(\Omega)]^d$ and $\nabla \cdot \mathbf{b} = 0$

Discontinuous Galerkin discretization

- Split Ω into a elements $\mathcal{T} = \{T\}$, and let $\mathcal{E} = \{e\}$ be the set of all edges in $\mathcal{T}$.

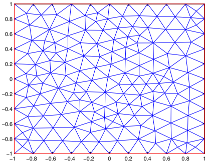

Figure : Example of a mesh on a unit square.

- Let $\mathcal{V}_H$ be the space of all discontinuous piecewise (bi)linear polynomials.

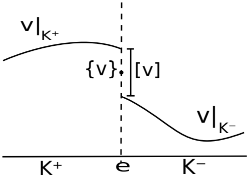

Figure : Example of $\{v\}$ and $[v]$

The bilinear form is defined by:

$$a_h(u,v) := a_h^{\mathrm{d}}(u,v) + a_h^{\mathrm{c\text{-}r}}(u,v).$$

where

$$a_h^{\mathrm{d}}(u,v) := (A\nabla_h u, \nabla_h v)_{L^2(\Omega)} + \sum_{e\in\mathcal{E}_h} \Big(\frac{\sigma_e}{h_e}([u],[v])_{L^2(e)} - (\{\nu_e \cdot A\nabla u\},[v])_{L^2(e)} - (\{\nu_e \cdot A\nabla v\},[u]_{L^2(e)}) \Big),$$

where σ_e is a constant and

$$a_h^{\mathrm{c\text{-}r}}(u,v) := (\mathbf{b}\cdot\nabla_h u + cu, v)_{L^2(\Omega)} + \sum_{e\in\mathcal{E}_h} (b_e[u],[v])_{L^2(e)} - \sum_{e\in\mathcal{E}_h(\Omega)} (\nu_e \cdot \mathbf{b}\{u\},[v])_{L^2(e)} - \sum_{e\in\mathcal{E}_h(\Gamma)} \frac{1}{2}((\nu_e\cdot\mathbf{b})u, v)_{L^2(e)},$$

where $b_e = |\nu_e \cdot \mathbf{b}|/2$.

- $a_h^{\mathrm{d}}(\cdot,\cdot)$ approximates the diffusion a interior penalty method.
- $a_h^{\mathrm{c\text{-}r}}(\cdot,\cdot)$ approximates the convection-reaction using upwind.

Discontinuous Galerkin discretization

- $a_h(\cdot,\cdot)$: symmetric interior penalty (SIPG) and upwind.
- The energy-norm is defined by

$$|||\cdot|||_h^2 = ||A^{1/2}\nabla_H \cdot||^2_{L^2(\Omega)} + \sum_{e\in\mathcal{E}} \left(\frac{\sigma}{H} + \frac{|\mathbf{b}\cdot\nu|}{2}\right)\|[\cdot]\|^2_{L^2(e)}$$

(One scale) DG method

Find $u_h \in \mathcal{V}_h$ such that

$$a_h(u_h, v) = F(v), \quad \text{for all } v \in \mathcal{V}_h.$$

(One scale) DG method ($\mathbf{b} = 0$)

Find $u_H \in \mathcal{V}_H$ such that

$$a_H(u_H, v) = F(v), \quad \text{for all } v \in \mathcal{V}_H.$$

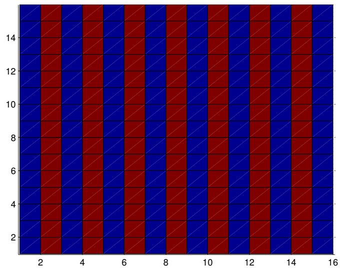

Figure : The coefficient A in the model problem.

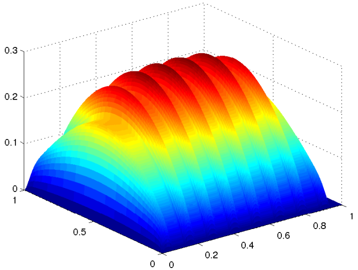

Figure : Reference solution.

(One scale) DG method ($\mathbf{b} = 0$)

Find $u_H \in \mathcal{V}_H$ such that

$$a_H(u_H, v) = F(v), \quad \text{for all } v \in \mathcal{V}_H.$$

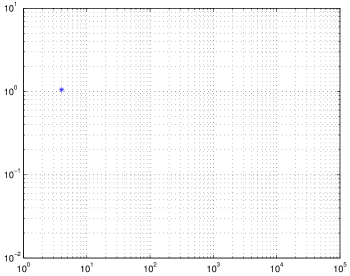

Figure : Energy norm with respect to the degrees of freedom.

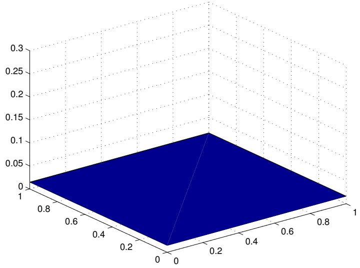

Figure : Solution obtained using the discontinuous Galerkin method.

(One scale) DG method ($\mathbf{b} = 0$)

Find $u_H \in \mathcal{V}_H$ such that

$$a_H(u_H, v) = F(v), \quad \text{for all } v \in \mathcal{V}_H.$$

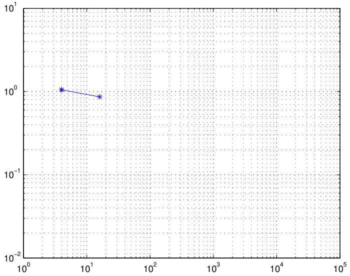

Figure : Energy norm with respect to the degrees of freedom.

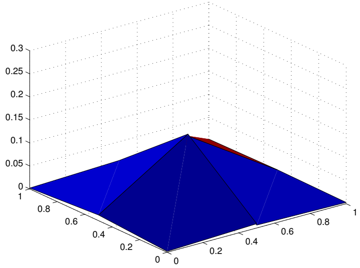

Figure : Solution obtained using the discontinuous Galerkin method.

(One scale) DG method ($\mathbf{b} = 0$)

Find $u_H \in \mathcal{V}_H$ such that

$$a_H(u_H, v) = F(v), \quad \text{for all } v \in \mathcal{V}_H.$$

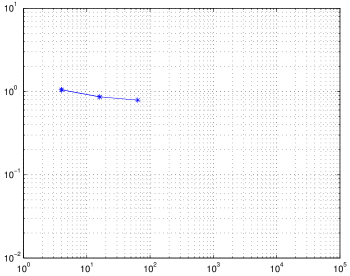

Figure : Energy norm with respect to the degrees of freedom.

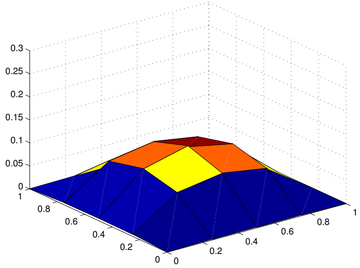

Figure : Solution obtained using the discontinuous Galerkin method.

(One scale) DG method ($\mathbf{b} = 0$)

Find $u_H \in \mathcal{V}_H$ such that

$$a_H(u_H, v) = F(v), \quad \text{for all } v \in \mathcal{V}_H.$$

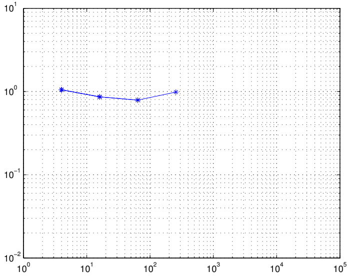

Figure : Energy norm with respect to the degrees of freedom.

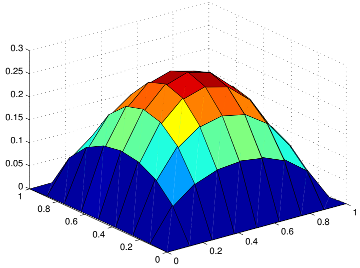

Figure : Solution obtained using the discontinuous Galerkin method.

(One scale) DG method ($\mathbf{b} = 0$)

Find $u_H \in \mathcal{V}_H$ such that

$$a_H(u_H, v) = F(v), \quad \text{for all } v \in \mathcal{V}_H.$$

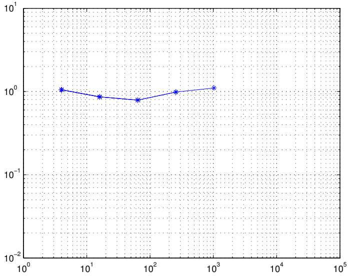

Figure : Energy norm with respect to the degrees of freedom.

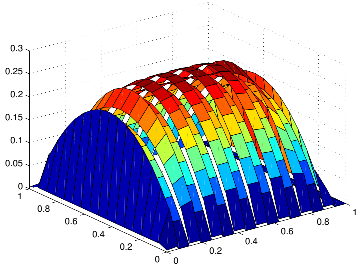

Figure : Solution obtained using the discontinuous Galerkin method.

(One scale) DG method ($\mathbf{b} = 0$)

Find $u_H \in \mathcal{V}_H$ such that

$$a_H(u_H, v) = F(v), \quad \text{for all } v \in \mathcal{V}_H.$$

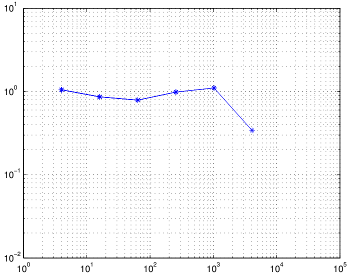

Figure : Energy norm with respect to the degrees of freedom.

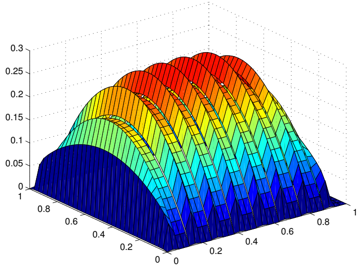

Figure : Solution obtained using the discontinuous Galerkin method.

(One scale) DG method ($\mathbf{b} = 0$)

Find $u_H \in \mathcal{V}_H$ such that

$$a_H(u_H, v) = F(v), \quad \text{for all } v \in \mathcal{V}_H.$$

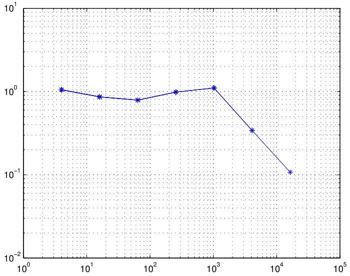

Figure : Energy norm with respect to the degrees of freedom.

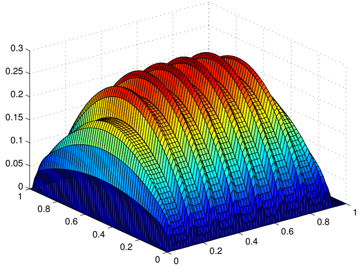

Figure : Solution obtained using the discontinuous Galerkin method.

(One scale) DG method ($\mathbf{b} = 0$)

Find $u_H \in \mathcal{V}_H$ such that

$$a_H(u_H, v) = F(v), \quad \text{for all } v \in \mathcal{V}_H.$$

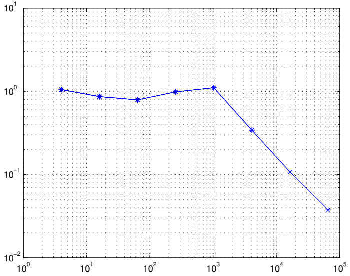

Figure : Energy norm with respect to the degrees of freedom.

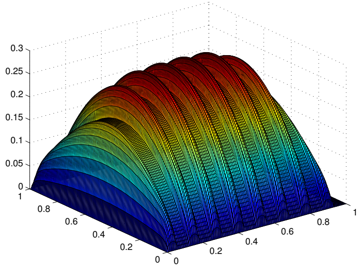

Figure : Solution obtained using the discontinuous Galerkin method.

Objective with the multiscale method

- Eliminate the dependency of A via a multiscale method i.e.,

$$|||u - u_H^{ms,L}||| \leq C_f H,$$

  where H does not resolve the variation in A
- Construct an adaptive algorithm to focus computational effort to critical areas (for the case with pure diffusion)

Incomplete list of other multiscale methods

- Variational multiscale method (VMS): [Hughes et al. 95]
- Multiscale FEM (MsFEM): [Hou-Wu 96]
- Heterogeneous multiscale method (HMM): [Engquist, E 03]
- Multiscale finite volume method: [Jenny et al. 03]
- Residual free bubbles: [Brezzi et al. 98]
- Upscaling techniques: [Durlofsky et al. 98]
- Equation free: [Kevrekidis et al. 05]
- Metric based upscaling: [Owhadi-Zang 06]
- Polyharmonic homogenization [Owhadi-Zang 12]
- Generalised MsFEM [Efendiev et al. 10]
- Mortar Multiscale Methods [Arbogast et al, 07]
- ...

Remarks

- Local approximations (in parallel) on a fine scale are used to modify a coarse scale space or equation

Local orthogonal decomposition

- Adaptivity [Larson, Målqvist 07], [Målqvist 11]
- Convergence analysis [Målqvist, Peterseim 14]
- Convergence analysis for DG [Elfverson et al. 13]
- Convection problem [Submitted]
- Semi-linear elliptic problem [Henning et al. 14]
- Egenvalue problem [Målqvist, Peterseim 14]
- Non-linear Schrödinger equation [Henning et al. 14]
- Petrov-Galerkin formulation [Submitted]
- Adpativity for DG [Elfverson et al. 13]
- ...

Remarks

- Builds on the idea of VMS
- Error analysis DOESN'T rely on assumptions such as scale separation and periodicity
- Error analysis does depend on the contrast, however numerical test show a very weak dependence

Local orthogonal decomposition

- Adaptivity [Larson, Målqvist 07], [Målqvist 11]
- Convergence analysis [Målqvist, Peterseim 14]
- Convergence analysis for DG [Elfverson et al. 13]
- Convection problem [Submitted]
- Semi-linear elliptic problem [Henning et al. 14]
- Egenvalue problem [Målqvist, Peterseim 14]
- Non-linear Schrödinger equation [Henning et al. 14]
- Petrov-Galerkin formulation [Submitted]
- Adpativity for DG [Elfverson et al. 13]
- . . .

Remarks

- Builds on the idea of VMS
- Error analysis DOESN'T rely on assumptions such as scale separation and periodicity
- Error analysis does depend on the contrast, however numerical test show a very weak dependence

Multiscale split

- Consider $\mathcal{V}_H$ and $\mathcal{V}_h$, such that $\mathcal{V}_H \subset \mathcal{V}_h$.
- Let Π_H be the L^2-projection onto $\mathcal{V}_H$.
- Define $\mathcal{V}^f(\omega) = \{v \in \mathcal{V}_h(\omega) : \Pi_H v = 0\}$.
- We have a L^2-orthogonal split; $\mathcal{V}_h = \mathcal{V}_H \oplus \mathcal{V}^f$.

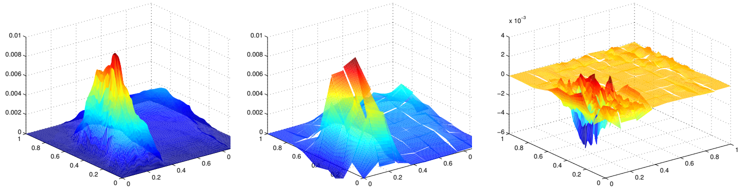

Figure : $u_h = u_H + u^f$

Corrected basis functions

- For each $\lambda_{T,j} \in \mathcal{V}_H$ we compute a corrector, find $\phi^L_{T,j} \in \mathcal{V}^f(\omega^L_T)$ such that

$$a_h(\phi^L_{T,j}, v_f) = a_h(\lambda_{T,j}, v_f), \quad \text{for all } v_f \in \mathcal{V}^f(\omega^L_T).$$

  where L indicates the size of the patch.
- Corrected space: $\mathcal{V}^{ms}_H = \text{span}\{\lambda_{T,j} - \phi^L_{T,j}\}$.
- We have a $a(\cdot,\cdot)$-orthogonal split; $\mathcal{V}_h = \mathcal{V}^{ms}_H \oplus \mathcal{V}^f$.

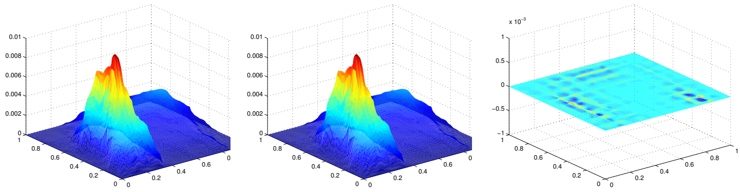

Figure : $u_h = u^{ms}_H + u^f$

Mesh patch

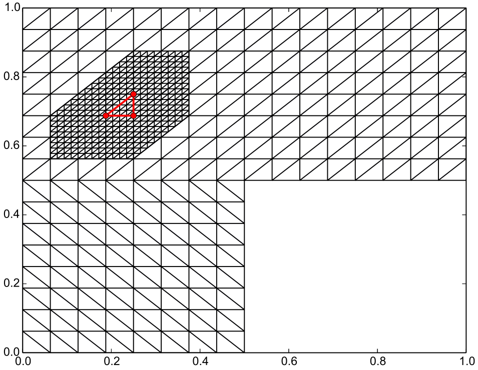

Examples of corrected basis functions

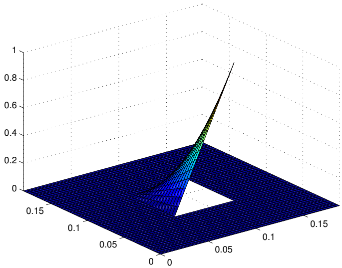

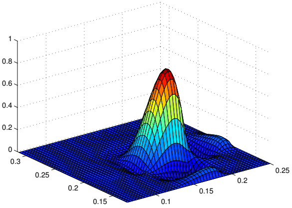

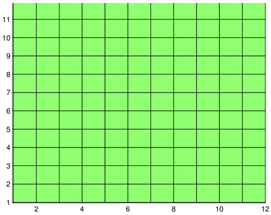

Examples of corrected basis functions

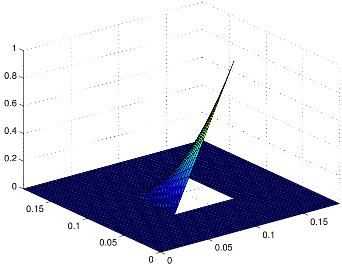

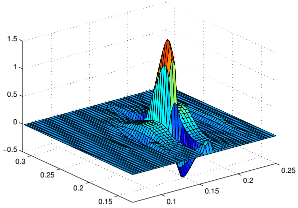

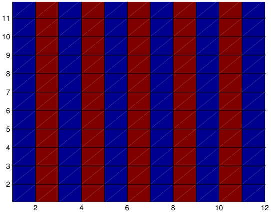

Examples of corrected basis functions

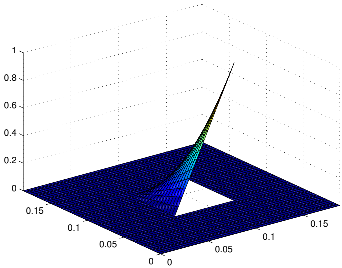

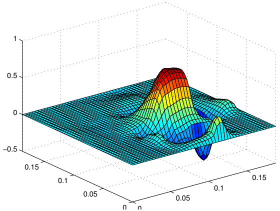

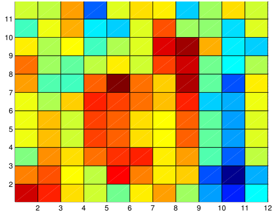

Example of corrected basis function

- With $\mathbf{b} = [0, 0]'$.

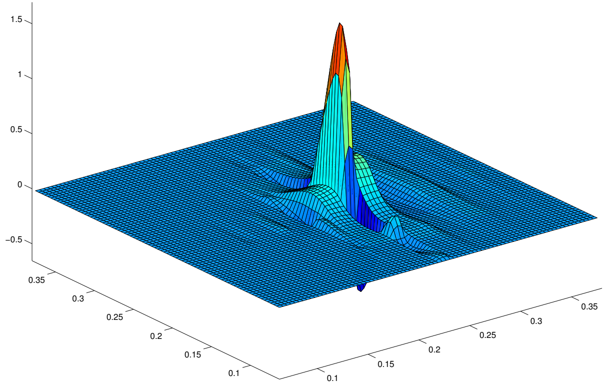

Example of corrected basis function

- With $\mathbf{b} = -[1, 0]'$.

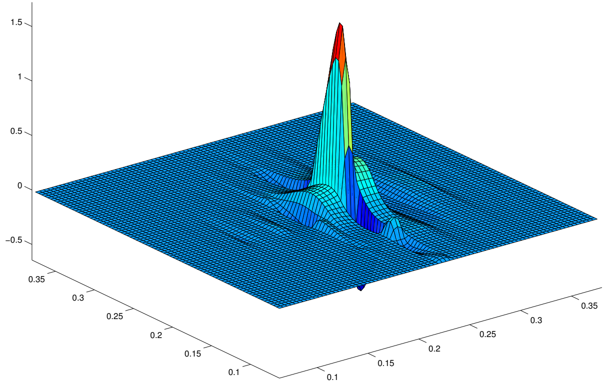

Example of corrected basis function

- With $\mathbf{b} = -[2,0]'$.

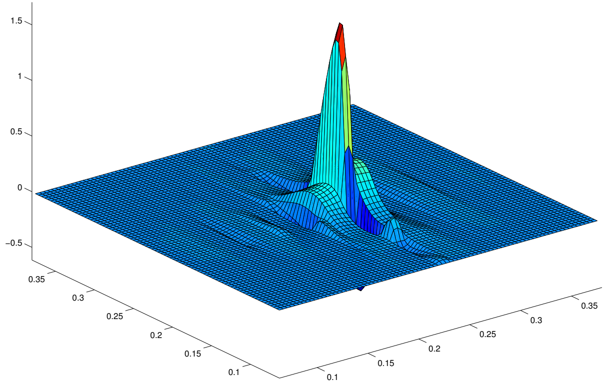

Example of corrected basis function

- With $\mathbf{b} = -[4, 0]'$.

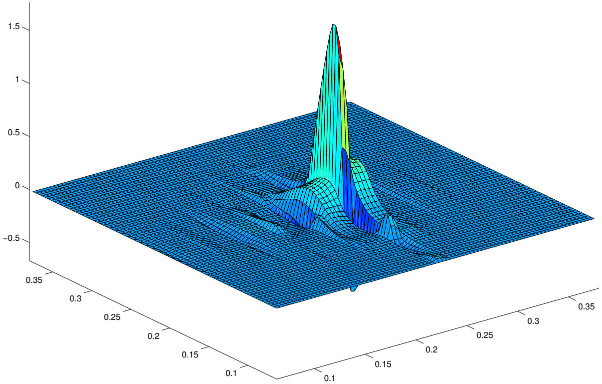

Example of corrected basis function

- With $\mathbf{b} = -[8, 0]'$.

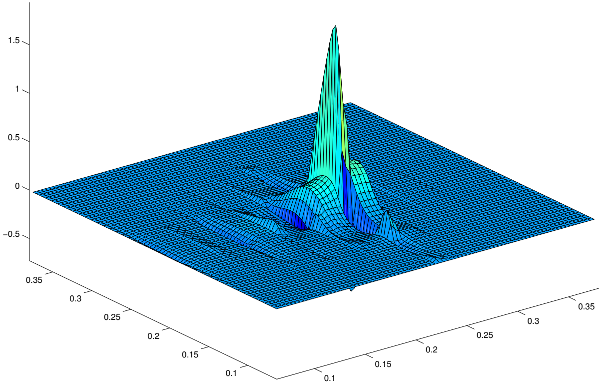

Example of corrected basis function

- With $\mathbf{b} = -[16, 0]'$.

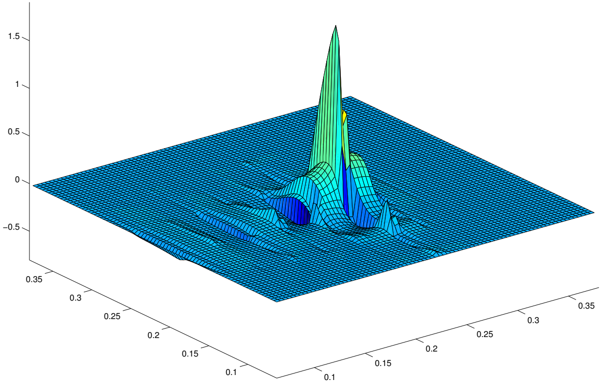

Discontinuous Galerkin multiscale method

Consider the problem: find $u_H^{ms,L} \in \mathcal{V}_H^{ms,L} = \text{span}\{\lambda_{T,j} - \phi_{T,j}^L\}$ such that

$$a_h(u_H^{ms,L}, v) = F(v), \quad \text{for all } v \in \mathcal{V}_H^{ms,L}.$$

- $\text{dim}\mathcal{V}_H^{ms,L} = \text{dim}\mathcal{V}_H$
- The basis function are solved independently of each other.
- Method can take advantage of periodicity.

A priori error bound

Under the assumption $\mathcal{O}(\|H\mathbf{b}\|_{L^\infty(\Omega)}/A_{min}) = 1$ it holds:

Lemma (Decay of corrected basisfunctions)

For $\phi_{T,j} \in \mathcal{V}^f(\omega_i^L)$, there exist a, $0 < \gamma < 1$, such that

$$|||\phi_{T,j} - \phi_{T,j}^L||| \lesssim \gamma^L |||\lambda_j - \phi_{T,j}|||.$$

Theorem

For $u_H^{ms,L} \in \mathcal{V}_H^{ms,L}$, there exist a, $0 < \gamma < 1$, such that

$$|||u - u_H^{ms,L}||| \lesssim |||u - u_h||| + ||H(f - \Pi_H f)||_{L^2} + H^{-1}(L)^{d/2}\gamma^L ||f||_{L^2}.$$

Choosing $L = \lceil C \log(H^{-1}) \rceil$ both terms behave in the same manor with an appropriate C.

Pure diffusion on L-shaped domain

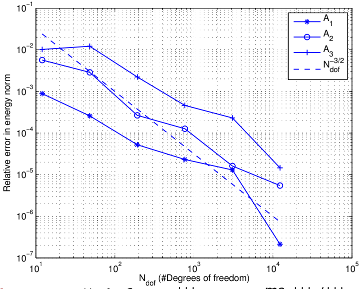

Figure : $\#dofs$ vs $|||u_h - u^{ms}_{H,L}|||/|||u_h|||$

- Choose $L = \lceil 2\log(\frac{1}{H}) \rceil$.
- Let the right hand side be: $f = 1 + sin(\pi x) + sin(\pi y)$.
- Let $H = 2^{-m}$ for $m = \{1, 2, 3, 4, 5, 6\}$.
- Reference mesh is 2^{-8}.

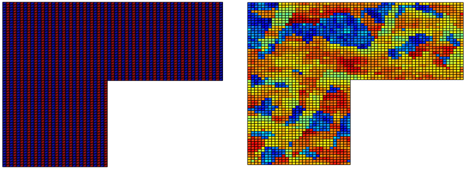

Figure : Permeabilities are piecewise constant on a mesh with size 2^{-5}, with ratio $A_{max}/A_{min} = \{10, 7 \cdot 10^6\}$

Numerical verification of the convergence

$$-\nabla \cdot A \nabla u + \mathbf{b} \cdot \nabla u = f \text{ in } \Omega,$$
$$u = 0 \text{ on } \partial\Omega.$$

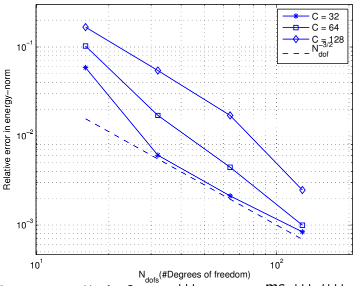

Figure : $\#dofs$ vs $|||u_h - u^{ms}_{H,L}|||/|||u_h|||$

- Let $A = 1$ and $\mathbf{b} = C[1, 0]'$ for $C = 32, 54, 128$.
- Choose $L = \lceil 2 \log(\frac{1}{H}) \rceil$.
- Let the right hand side be: $f = 1 + sin(\pi x) + sin(\pi y)$.
- Let $H = 2^{-m}$ for $m = \{2, 3, 4, 5\}$.
- Reference mesh is 2^{-7}.

$$-\nabla \cdot A\nabla u + \mathbf{b} \cdot \nabla u = f \text{ in } \Omega,$$
$$u = 0 \text{ on } \partial\Omega.$$

- Let $\mathbf{b} = [1, 0]'$.

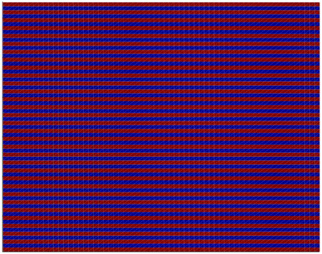

Figure : Diffusion coefficient A, $A_{max}/A_{min} = 100$ and $A_{min} = 0.01$.

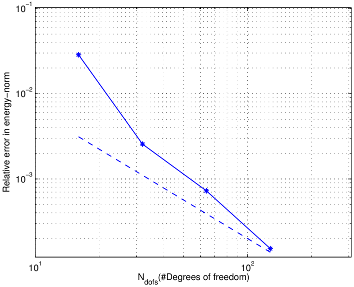

Figure : $\#dofs$ vs $|||u_h - u^{ms}_{H,L}|||/|||u_h|||$

$$-\nabla \cdot A\nabla u + \mathbf{b} \cdot \nabla u = f \text{ in } \Omega,$$
$$u = 0 \text{ on } \partial\Omega.$$

- Let $\mathbf{b} = [512, 0]'$.

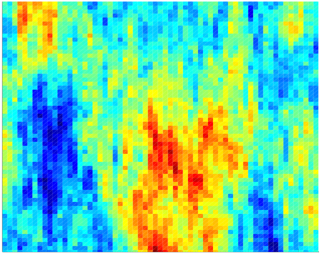

Figure : Diffusion coefficient A with $A_{max}/A_{min} \sim 10^5$ and $A_{min} = 0.05$.

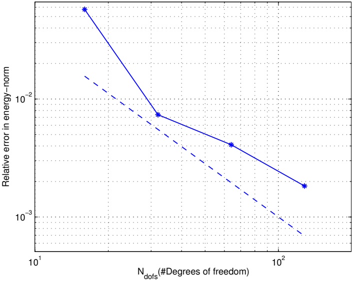

Figure : $\#dofs$ vs $|||u_h - u^{ms}_{H,L}|||/|||u_h|||$

Petrov-Galerkin DG-LOD

Consider the problem: find $u_H^{ms,L} \in \mathcal{V}_H^{ms,L} = \text{span}\{\lambda_{T,j} - \phi_{T,j}^L\}$ such that

$$a_h(u_H^{ms,L}, v) = F(v), \quad \text{for all } v \in \mathcal{V}_H = \text{span}\{\lambda_{T,j}\}$$

Same as before:

- $\dim \mathcal{V}_H^{ms,L} = \dim \mathcal{V}_H$
- The basis function are solved independently of each other.
- Method can take advantage of periodicity.

Pros

- Quadrature for the coarse system becomes easier, i.e., $a_h(\lambda_{T,j} - \phi^L_{T,j}, \lambda_{T,j})$
- Sparser coarse system
- Less memory consumption, after being computed the correctors $\phi^L_{T,j}$ can be disgarded.

Cons

- Non-symmetric coarse system
- Harder (missing) analysis

Adaptivity and a posteriori error bound ($\mathbf{b} = 0$)

Theorem (A posteriori error bound)

Let $u_H^{ms,L}$ be the multiscale solution, then

$$|||u - u_H^{ms,L}||| \lesssim \left(\sum_{T \in \mathcal{T}_H} \rho_{h,T}^2(u_H^{ms,L}) \right)^{1/2} + \left(\sum_{T \in \mathcal{T}_H} \rho_{L,\omega_T^L}^2(u_H^{ms,L}) \right)^{1/2}.$$

- $\rho_{L,\omega_i^L}^2$ measures the effect of the truncated patches.
- $\rho_{h,T}^2$ measures the effect of the refinement level.

Adaptivity

- We consider the permeabilities

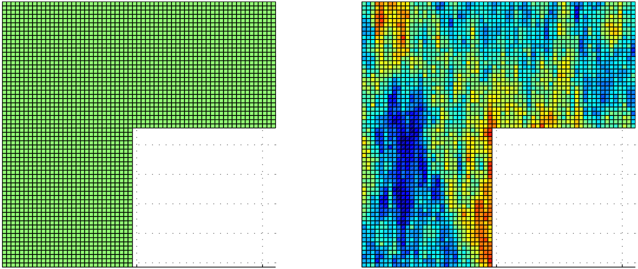

Figure : Permeabilities *One* left and *SPE* right.

- Using a refinement level of 30% we have.

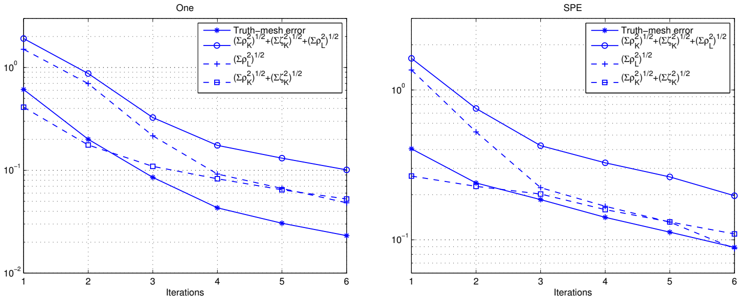

Figure : Convergence plot for *One* left and *SPE* right.

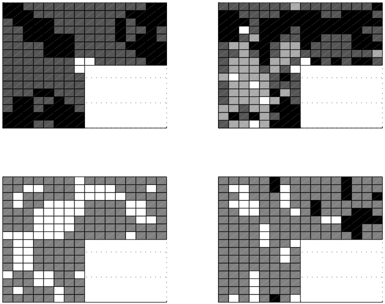

Figure : One (left) and SPE (right). The level of refinement (upper) and size of the patches (lower).

Perspective towards Two-Phase flow

Buckley-Leverett system

$$-\nabla \cdot (K\lambda(S)\nabla p) = q \text{ and } \partial_t S + \nabla \cdot (f(s)\mathbf{v}) = q_w$$

is solved using IM(plicit)P(ressure)E(plicit)S(aturation)

- K is the hydraulic conductivity
- $\lambda(S)$ is the total mobility (essentially macroscopic)
- and $\mathbf{v} = -K\lambda(S)\nabla p$ is obtained from the pressure equation

- Coarse mesh $H = 2^{-5}$ and fine mesh $h = 2^{-8}$.
- Boundary condition $p = 1$, on left boundary $p = 0$ on right boundary, and $K\lambda(S)\nabla p = 0$ otherwise.
- Prepossessing step: compute the basis corrected basis using $\lambda(S) = 1$

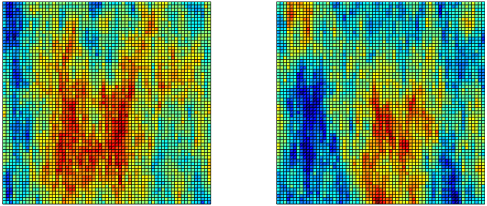

Figure : K_1 $(A_{max}/A_{min} \approx 5 \cdot 10^5)$ left and K_2 $(A_{max}/A_{min} \approx 4 \cdot 10^5)$ right on a mesh with size 2^{-6}.

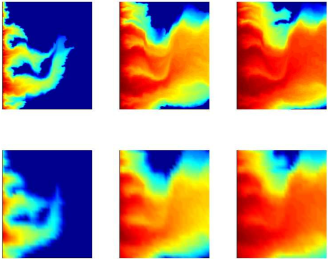

Figure : Saturation profile K_1 for T_1, T_2, and T_3.

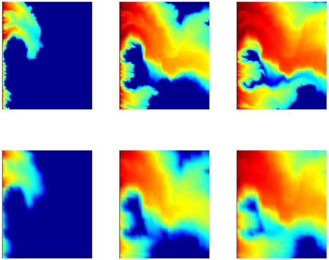

Figure : Saturation profile K_2 for T_1, T_2, and T_3.

Data	$\|e(T_1)\|_{L^2(\Omega)}$	$\|e(T_2)\|_{L^2(\Omega)}$	$\|e(T_3)\|_{L^2(\Omega)}$
1	0.088	0.073	0.070
2	0.058	0.087	0.079

Table : Error in relative L^2-norm, $e(T) = S(T) - S^{\mathrm{ref}}(T)$.

On going work - LOD on complex geometries

- Construt a method which with textbook convergance which do not resolve the boundary.
- Add correctors locally to handel e.g. singularites and/or interfaces.

Preliminary numerical results

- Homogeneous Dirichlet boundary condition
- Choose $L = \lceil \log(\frac{1}{H}) \rceil$.
- Let $H = \sqrt{2} \cdot 2^{-m}$ for $m = \{2, 3, 4, 5\}$
- Reference mesh is $h = \sqrt{2} \cdot 2^{-8}$
- Holes has radius $r = \{0.01, 0.03\}$ $(\{2^{-6.6439}, 2^{-5.0589}\})$
- $f = \cos(8\pi x)\cos(8\pi y) + 0.5$

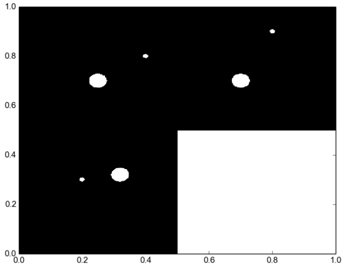

Figure : Computational domain.

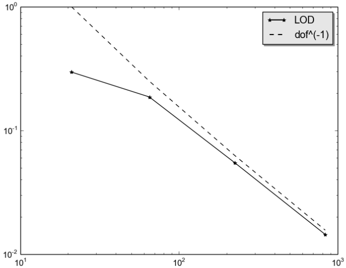

Figure : Error estimate.

- D. Elfverson, G. H. Georgoulis, and A. Målqvist An adaptive discontinuous Galerkin multiscale method for elliptic problems. *Multiscale Model. Simul.*.
- D. Elfverson, G. H. Georgoulis, A. Målqvist and D. Peterseim Convergence of discontinuous Galerkin multiscale methods. *SIAM J. Numer. Anal.*.
- D. Elfverson A discontinuous Galerkin multiscale method for convection-diffusion problems. *Submitted*.
- D. Elfverson, V. Ginting, P. Henning On Multiscale Methods in Petrov-Galerkin formulation. *arXiv:1405.5758, submitted*.